Fuzzy Logic Compliance Adaptation for an Assist-as-Needed Controller on the Gait Rehabilitation Exoskeleton (GAREX)

Bin Zhong#, Jinghui Cao#, Kaiqi Guo, Andrew McDaid, *Member, IEEE,* Yuxin Peng, Qing Miao, ShengQ. Xie, *Senior Member, IEEE,* Mingming Zhang*, *Member, IEEE*

Abstract: **Assist-as-needed control strategy is an emerging approach to improve the effectiveness of gait rehabilitation training. We have proposed a pneumatic muscle (PM) driven Gait Rehabilitation Exoskeleton (GAREX) implemented with a multi-input-multi-output (MIMO) sliding mode control system to actively adjust the assistance level provided during gait rehabilitation. To realize the assist-as-needed control strategy, a specific algorithm is imperative to assess the active participation or effort of wearers and adapt the amount of assistance accordingly. We sought to establish a fuzzy logic compliance adaptation (FLCA) controller to form a novel cascade control system. We evaluated the feasibility of implemented FLCA controller on the performance of adjusting the compliance of GAREX's knee joint according to the online assessment of the wear's active participation level once in every gait cycle. Using controlled, treadmill-based walking tests involved three healthy subjects, we demonstrate that FLCA controller could effectively distinguish the capability/effort levels of wearers and enable the exoskeleton to adapt the knee joint compliance accordingly. Obtained results reveal that FLCA controller can collaborate well with MIMO sliding mode controller in a system and indicate the novel method of realizing assist-as-needed concept with the pneumatic muscle powered mechanisms.**

Index Terms: **Fuzzy logic, pneumatic muscle, compliance adaptation, gait rehabilitation, assist-as-needed.**

I. Introduction

Trajectory tracking control systems are the foundation for gait rehabilitation robotics. This control strategy is more suitable for patients with severe gait disorder or at the initial stage of gait rehabilitation, who need repetitive gait training referred to a predefined gait trajectory. However, pure trajectory tracking control strategy may not be optimal for providing effective gait rehabilitation since it could decrease the subject's motor output, effort, energy consumption and/or attention [1]. Then the assist-as-needed (AAN) training strategy, which indicates the robotic devices only supply as much effort as a wearer needs to accomplish training tasks by assessing his/her participation level in real-time, is attracting more interests of researchers. The ANN strategy encourages the voluntary participation of the wearer , and earlier studies have evaluated the performance of active (voluntary) and passive training in rehabilitation [2-6], and the results demonstrated that higher voluntary participation of subjects can contribute to superior rehabilitation outcomes.

Mainly two types of implementations of the AAN concept have been identified. One is through adapting the desired speed or gait trajectory [7, 8] and the other is through impedance or admittance related control strategies [9, 10]. Impedance related controllers have been implemented on different platforms, especially the ones with stiff actuators, while extra force sensors and modeling work are needed to enable them possess expected compliant behaviors. For the robots driven by series elastic actuators, the compliant and back-drivable actuators eased the implementation of impedance control, especially the low/zero impedance control mode. However, during impedance control, the actuators act as force/torque source. Stability may become an issue if the controller cannot react fast and accurate enough to adjust the force/torque based on the robot kinematics. Moreover, the adaptive impedance controller developed to the PM-driven robot [10] was similar to the algorithm implemented to the motor-driven system [9]. Whereas, due to the process of in-/deflation and nonlinearity, the pneumatic muscles may not be a high-precision force source for impedance control. Hence, the bandwidth of such PM based adaptive impedance control system could be very limited. In comparison, the robust trajectory tracking controller is preferred to ensure the stability of the control system of PM-driven robots. Conventional robotic trajectory tracking gait training ignored the wearer' active participation, but this can be improved by utilizing the intrinsic compliance of the PM actuators to vary the extent of provided guidance. Then challenge falls on the simultaneous control of both joint space position and compliance. The controllers presented in [11] only had closed-loop control of the position and the compliance was calculated through an open-loop model based on the PMs. In this paper, we have proposed an adaptive compliance control system based on the variable stiffness property of PM to achieve AAN gait rehabilitation.

When developing an AAN control strategy, it is crucial to assess a wear's capability or participation as to adjust the assistance level provided by the rehabilitation robot. The most commonly used as well as easily implemented participation assessing method is via gait kinematics or more specific derivations from the reference trajectories, including invariant impedance control controllers [12], force field

This manuscript was submitted August 15, 2019. This work was supported in part by National Natural Science Foundation of China under Grant 6190021385, in part by Guangdong Provincial Natural Science Foundation under Grant 2020A151501401, in part by Guangdong Research Program under Grant 2019ZT08Y191 and the University of Auckland Doctoral Scholarship. (*Corresponding author: Mingming Zhang.)

Bin Zhong and Jinghui Cao devoted equally to this work.

Bin Zhong (11955001@mail.sustech.edu.cn), Kaiqi Guo (11930454@mail.sustech.edu.cn), and Mingming Zhang* (zhangmm@sustech.edu.cn) are with the Department of Biomedical Engineering, Southern University of Science and Technology, Shenzhen 518055, China.

Jinghui Cao (jcao027@aucklanduni.ac.nz) and Andrew McDaid (andrew.mcdaid@auckland.ac.nz) are with the Department of Mechanical Engineering at the University of Auckland, New Zealand.

Yuxin Peng is with the Department of Physical Education and Sports Science, Zhejiang University, Hangzhou, China. (e-mail: yxpeng@zju.edu.cn).

Qing Miao is with the School of Mechanical and Electrical Engineering, Wuhan University of Technology, Wuhan, China. (e-mail: miaoqing0702@whut.edu.cn).

ShengQ. Xie is with the School of Electronic and Electrical Engineering, University of Leeds, Leeds, UK. (e-mail: s.q.xie@leeds.ac.uk).

controllers [13, 14] and impedance adaptation algorithms via gait velocities [15]. The interaction force/torque between the exoskeleton and human lower limb has also been used to estimate the subject's participation level during gait rehabilitation. Jezernik et al. [8] developed gait pattern adaptive algorithms to online optimize the reference trajectory of the gait orthoses based on the patient's walking capability. Impedance adaptive controllers based on interaction force/torque measurement have also been reported in [9, 10]. The adaption algorithms presented in [8] and [10] rely on the models of the exoskeleton and/or the biomechanical properties of the human limb attached. The complexity of modeling work and the possible modeling inaccuracy make such controllers less practical in clinical scenarios.

Fuzzy logic provides an option for controlling complicated or nonlinear systems with uncertainties. Fuzzy logic controllers are developed based on system behaviors and usually do not require models of the systems. Benefitted from such properties, they have been widely used in the field of rehabilitation robotics, where the human factor is commonly regarded to be difficult to model accurately. Chang et al. [16] reported an adaptive self-organizing fuzzy sliding mode (SM) trajectory control system for a PM driven two-degree-of-freedom serial robot manipulator. Xie and Jamwal [17] developed an iterative fuzzy controller for a pneumatic muscle (PM) driven parallel ankle rehabilitation robot. Besides trajectory tracking control, fuzzy logic has also been utilized to control impedance/admittance magnitudes of various robotic rehabilitation systems. Tran et al [15] developed a fuzzy logic-based variable impedance controller for a lower limb exoskeleton. Different fuzzy rules have been developed for the stance and swing phases to achieve optimized control results. Yang et al. [18] implemented a fuzzy logic tuner for the impedance controller of a cable-driven upper limb rehabilitation robot. Ayas and Altas [19] applied fuzzy logic adaptive admittance control to a parallel ankle rehabilitation robot. The fuzzy impedance adaptation controllers reported in [15, 18] only utilized kinematic data as inputs to the fuzzy logic. The admittance controller in [19] only used the interaction force as the input.

The GAREX platform (shown in Fig.1) and the detailed MIMO sliding mode control system that enables both task-specific gait training and the control of the joint compliance have been introduced in [20]. The controllable compliance allows the control of the assistance level provided by the exoskeleton. To realize the assist-as-needed control strategy, a specific algorithm is essential to assess the active participation or effort of wearers and adapt the amount of assistance accordingly. We sought to establish a fuzzy logic compliance adaptation (FLCA) controller to achieve this purpose. A fuzzy logic compliance adaption controller benefits this nonlinear system simultaneously with the capability of dealing with multivariable inputs. This method also allows designing the adaptation law using predefined training principles directly from clinical practice in natural language terms. Using this compliance controller, the assist-as-needed training has been realized, and we demonstrate the contributions of this work as following: 1) this is a novel approach to establish a cascade control system with fuzzy logic and sliding mode control for PM driven rehabilitation robots; 2) proposed fuzzy logic controller is model-free and robust.

This paper is organized in the following order. First is the presentation of the improved hardware design with the human-exoskeleton interaction force sensing instrumenttation. This is followed by the development process of the fuzzy logic compliance adaption algorithm. The next section will be on the experimental validation of the system with three healthy subjects. The discussion and conclusions are presented at last.

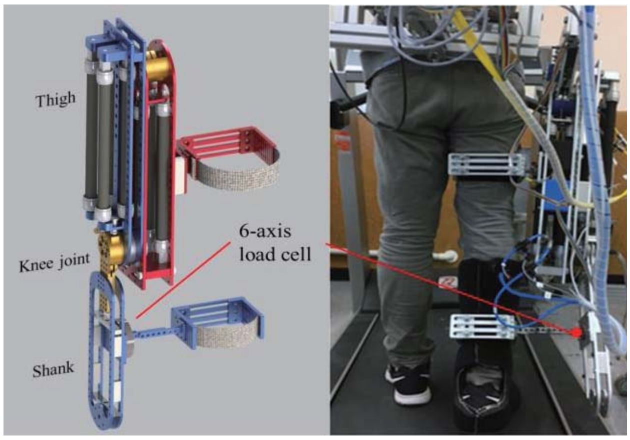

Fig 1. The developed GRAEX system and the illustration of the treadmill-based walking tests. The 6-axis load cell is implemented at the shank.

II. METHODS

A. GAREX System

The GAREX system has been previously reported in [20]. Four 3/5 analog valves (FESTO: MPYE-5-1/8-HF-010-B) were adopted, similar to that reported in [6], two for each actuated joint. The pneumatic flow through the valve can be controlled by changing its orifice area which depends on the input voltage. Two magnetic encoders (AMS: AS5048B) and four pressure transducers (FESTO: SPTE-P10R-S6-V2.5K) are adopted to feedback joint space kinematics and actuator pressures for the control system. A MyRIO platform by National Instrument is employed for data acquisition and real-time control processing. MyRIO consists of one micro-processor and one FPGA module. Data acquisition and signal processing are performed through the MyRIO's FPGA module at a rate of 1 kHz. The real-time controller runs on the micro-processor at a rate of 100 Hz. A custom printed circuit board was also designed for physical hardware interfacing the MyRIO.

Healthy subjects with no current lower limb injury were recruited to be involved in the experiments. Ethical approval for the experiments was granted by the University of Auckland Human Participants Ethics Committee (014970). Written informed consent had been obtained from all the participants before conducting any experiments.

B. Interaction Torque Sensing

Interaction force/torque measurements have been utilized for the assessment of subjects' effort or active participation during robotic gait rehabilitation. A 6-axis load cell was employed in this study for human-robot interaction force sensing. It was installed between the shank segment of the exoskeleton and the brace for the human shank, as shown in Fig.1. Since the load cell is the only link between shank segments of the exoskeleton and the training subject, the sensed forces and torques are thus the interactive forces and torques. In this application, only the interaction knee joint torque in the sagittal plane is of the researcher's interest. The joint torque can be calculated simply by the product of the interactive force along the y-axis and its moment arm relative to the sagittal plane rotation of the knee joint.

C. Relation of Interactive Torque and Subject Participating Level

The sensed interaction forces have been used as an indication of the subject's effort during rehabilitation training [9]. Higher interaction force was regarded as less effort from the subject to walk in a desired gait pattern. Hence, to ensure the desired gait pattern can be achieved the higher impedance should be induced. In contrast, lower interaction force indicated more effort from the subject to synchronize his/her leg movements to the desired trajectories of the rehabilitation robot. Hence, lower impedance is adapted.

Pilot experiments were designed to investigate how a subject's effort is reflected by the various sensor measurements of the system. The experiments were conducted with a neurologically intact subject (male, 185 cm, 100 kg) with no lower limb injury. The MIMO sliding mode controller presented in [20] was adopted to control the exoskeleton. Both the hip and knee joints of GAREX were actively controlled to guide the subject to walk on the treadmill at the speed of 1.5 km/h. The average PM pressures of the two actuated joints were regulated to 270 KPa based on the previous experience. Different patients' capabilities or participating levels were simulated through three experiments. In the first experiment, the subject was requested to actively engage the gait training by following the robotic guidance to walk in the desired trajectory. The second experiment simulated the no effort scenario. The subject tried to relax the leg attached to the exoskeleton as much as possible let the exoskeleton provide the torque required to produce the reference gait pattern. In the third experiment, stiff leg or undesired leg movements (spasms) were simulated. The subject was asked to slightly oppose the robotic guidance during the swing phase of every gait cycle. While this was subjective, it still gave the pilot data necessary to develop our controller. The experimental results of the three experiments are shown in Fig.2.

To compare the differences of the three experimental scenarios, root means square (RMS) values of the trajectory tracking error and the interaction torque were calculated for every gait cycle period during the experiments and shown in the result plots, the results showed the position tracking error for three experiments are around 0.1 rad, 0.12 rad, and 0.19 rad, respectively. These results indicated the GAREX system performed a comparable, if not better than, position tracking to existing gait rehabilitation devices [21-24]. It can be summarized that the subject's active participation or effort leads to better trajectory tracking accuracy and less RMS interaction torque over a gait cycle period compared to the experiment when the subject tried to relax and make no effort. On the other side, when the subject deliberately opposed the guidance of the exoskeleton, a larger overall trajectory error has resulted. The robotic system hence increased the control effort to drive the knee joint back to the desired trajectory, which thus led to higher interaction torque.

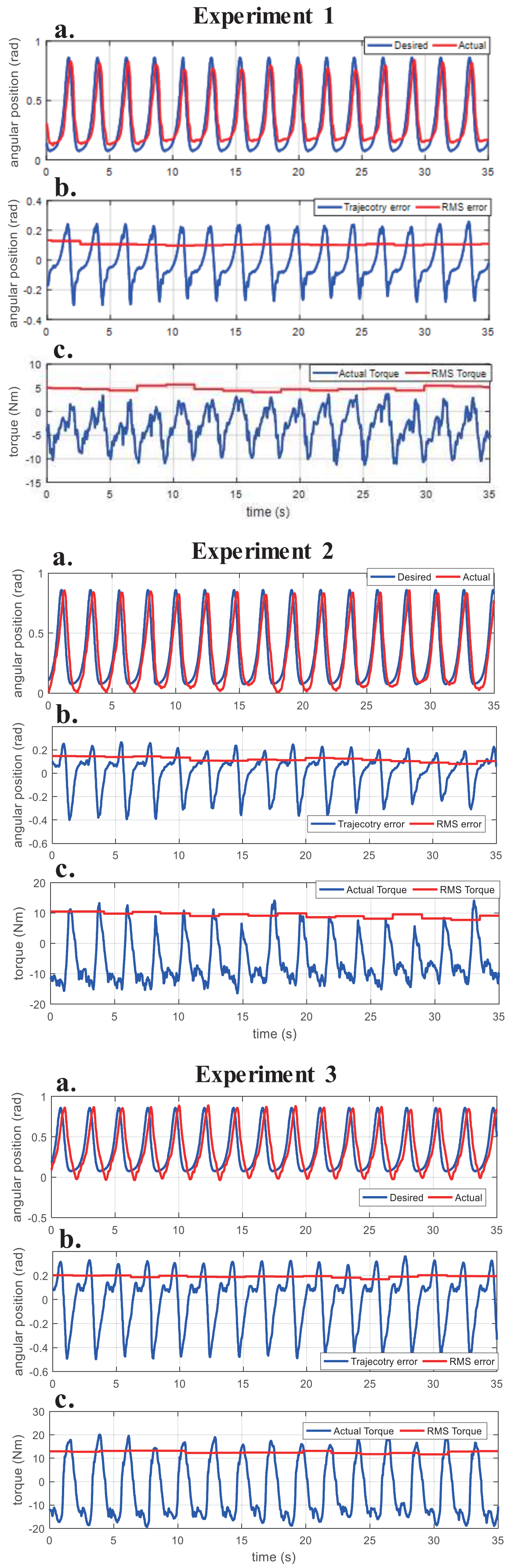

Fig 2. Experimental results of measured human-robot interaction forces in three designed cases under a constant pressure at 270 KPa. In these figures: (a) Desired and actual knee joint trajectories versus time plot; (b) Plots of trajectory error and RMS trajectory error over every gait cycle; (c) Plots of interaction torque and RMS interaction torque over every gait cycle.

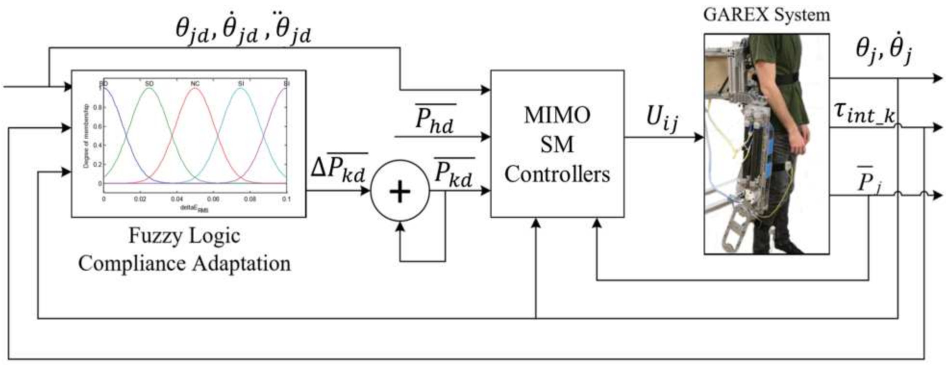

Fig 3. The fuzzy compliance adaptive control system block diagram of GAREX. In this figure, $\boldsymbol{i} = \boldsymbol{F}, \boldsymbol{E}$ (flexion, extension) and $\boldsymbol{j} = \boldsymbol{h}, \boldsymbol{k}$ (hip, knee); $\boldsymbol{U_{ij}}$ is the input to the plant or the voltages fed into the corresponding analogue valves; $\boldsymbol{\tau_{int\_k}}$ is the interaction torque of the knee joint; $\overline{\boldsymbol{P}}_{\boldsymbol{j}}$ is the average pressure of the antagonistic PMs of the corresponding joint; parameters with the subscript $\boldsymbol{d}$ indicate desired values; and $\Delta\overline{\boldsymbol{P}}_{\boldsymbol{jd}}$ is the increment to the desired average pressure of the antagonistic PMs of the joints.

D. FLCA controller

The goal of the adaption algorithm is to encourage active participation of training subjects by only providing as much assistance as he/she needed to walk in desired trajectories. From the experiments conducted in the last section, the general principles for compliance adaptation can be summarized as follows (the speed of treadmill is set at 1.8 km/s, and the stride frequency is around 2.2 s/gait cycle): (1) low interaction torque with low trajectory error. This case demonstrates that the subject possesses good walking capability and less robotic assistance is needed. Let the compliance level stay to where it is; (2) low interaction torque with high trajectory error. This case demonstrates that the subject cannot walk in the desired pattern and more robotic assistance is needed. Compliance level needs to be reduced for more guidance; (3) high interaction torque with low the trajectory error. This case demonstrates that the subject is going great with high robotic assistance. Compliance level should be reduced to encourage more participant of the subject; (4) high interaction torque with high the trajectory error. The case demonstrates that the subject cannot walk in the desired pattern but the exoskeleton has already been providing a lot of assistance. Let the compliance level temporally stay where it is.

It is understood that any change in compliance will influence both the interaction torque and the trajectory tracking error. The change in interaction torque or trajectory error will affect each other. A fuzzy logic compliance adaptation controller is a good candidate for such a complex system and hence developed to implement the AAN rehabilitation concept. The block diagram of the control system is presented in Fig.3.

The frequency of the compliance adaptation processing was set to be the gait cycle frequency of the exoskeleton. There are two main reasons for this decision. Firstly, the compliance adaptation is based on the subject's performance over a past period rather than a certain instant. Hence, it is not necessary to run the compliance adaptation controller at the same frequency as the MIMO sliding mode controller (100 Hz). Secondly, the trajectory error and interaction torque distributions over a gait cycle are not homogeneous. If the sampling periods contain different parts of a gait cycle, it is difficult to find standards to evaluate the subject's effort during those sampling periods. Hence, it is a good practice to set the sampling period to be integer multiples of the gait

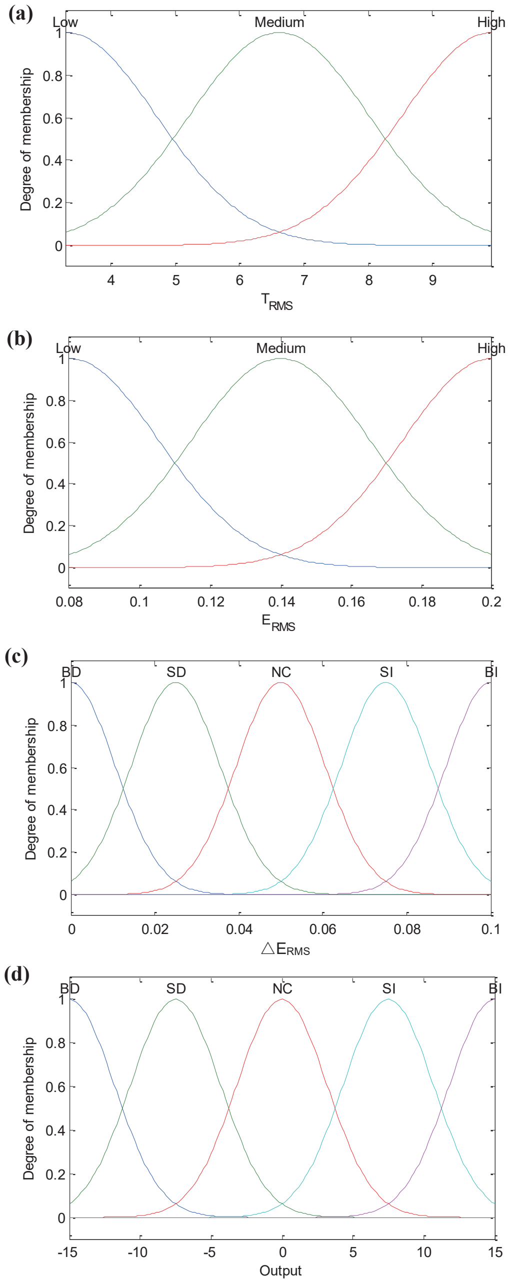

Fig 4. The membership functions of the input variables. (a) The RMS value of the interaction torque (N/m) over a gait cycle; (b) The RMS value of the tracking error(rad) over a gait cycle; (c) The change of the tracking error between the current and previous gait cycle; (d) The output membership function of the FLCA controller.

cycle period. In this application, the sampling period was chosen to be the same as the gait cycle period.

There are three major stages of the fuzzy logic controller implementation:

1. Define the inputs/outputs: As shown in Fig. 3, the RMS values of the knee joint trajectory error (θ_k) and the interaction torque (τ_{int_k}) of the past gait cycle are two of the inputs of the fuzzy logic controllers. The difference between the RMS trajectory errors of the current and the last gait cycles is calculated as the third input of the controller, shown in (1).

$$\Delta\theta_k = \theta_{k(n)} - \theta_{k(n-1)} \qquad (1)$$

this input is utilized to reflect if the system's trajectory tracking performance is improving. The output of the controller is the increment ($\Delta\overline{P}_{kd}$) to the desired average pressure of the knee joint.

2. Perform fuzzification: Fuzzification was performed to acquire input and output membership functions. The fuzzification of the inputs and outputs was through the membership functions shown in Fig.4. The crisp input and output values are converted into linguistic variables and membership values. The fuzzy set of each input or output is determined using the membership functions which are normally distributed around its center. There are three linguistic variables or membership functions (low, medium and high) each for the trajectory error and interaction torque inputs. The third input variable ($\Delta\theta_k$) and the output variable ($\Delta\overline{\boldsymbol{P}}_{jd}$) each can be further divided into five linguistic variables, which are BD (big decrease), SD (small decrease), NC (no change), SI (small increase) and BI (big increase). The center value of the Gaussian-shaped membership functions was tuned and finalized through experiments with the developed FLCA enabled control system. For certain input values, the membership degrees for the linguistic variables of each input can be calculated with membership functions as μ_{a_i} $(i = 1, 2, 3)$, μ_{b_i} $(i = 1, 2, 3)$, μ_{c_i} $(i = 1, 2, 3, 4, 5)$ for 3 levels of the inputs of the trajectory error, and interaction torque, and 5 levels of change in trajectory error, respectively.

3. Inference process: This process generates the membership degrees of the output linguistic variables based on the fuzzified inputs. The key to the inference process is the development of the fuzzy rules. The fuzzy rules are to reflect the expectation of compliance adaptation by linking the linguistic variables with a combination of input linguistic variables. Table I exhaustively listed the fuzzy output generated by all 45 input combinations with five sub-tables. The fuzzy rules were first developed by the four principles stated at the beginning of this section and further tweaked through experiments. The well-known Mamdani's max-min method [25] is used for the inference process. From Table I, it can be seen that a certain amount of combinations of input linguistic variables that lead to the same output linguistic variable. To calculate the membership degree of the output linguistic variable, the membership degree resulted by each of the possible combinations is calculated first as in (2).

$$\mu_{d\_i(j)} = min(\mu_{a\_x}, \mu_{b\_y}, \mu_{c\_z}) \\ \text{with } (j = 1,2,\dots,n) \qquad (2)$$

where n is the number of possible combination of input linguistic variables that lead the ith output linguistic variable; μ_{a_x}, μ_{b_y}, μ_{c_z} are the membership degrees of the input linguistic variables in that specific combination. The minimum of μ_{a_x}, μ_{b_y}, μ_{c_z} is calculated and assigned to $\mu_{d\_i(j)}$. The membership degrees of the output linguistic variables are calculated as the maximum of all the possible values ($\mu_{d\_i(j)}$) in (3).

$$\mu_{d\_i} = max(\forall_{j \in (1,2,\dots,n)} \mu_{d\_i(j)}) \qquad (3)$$

The defuzzification stage maps the conversion from the degrees of the output membership function to the non-fuzzy controller output. The center of area method is used for this process. The controller was developed with the help of the Fuzzy System Designer with the LabVIEW software package. The designed FLCA controller was programmed in LabVIEW and run on the MyRIO real-time control platform.

TABLE I. The rule table for the FLCA.

$\tau_{int\_k\_RMS}$	θ_{k_RMS}														
	L	M	H	L	M	H	L	M	H	L	M	H	L	M	H
L	SD	NC	SI	NC	NC	SI	NC	SI	BI	NC	SI	BI	SI	SI	BI
M	SD	SD	SI	SD	NC	SI	SD	SI	SI	NC	SI	SI	NC	SI	BI
H	BD	SD	NC	BD	SD	SI	BD	NC	SI	SD	NC	SI	NC	SI	SI

Note: L: Low, M: Medium, H: High, grids shaded in different colors represent different levels of the inputs $\Delta\theta_{k\_RMS}$ and τ_{int_k}, light grey for "BD", dark grey for "SD", yellow for "NC", blue for "SI", and green for "BI".

III. Experiments and Results

Experiments were conducted with three healthy subjects (Subject A: male, 172 cm, 62 kg; Subject B: male, 185 cm, 100 kg; Subject C: male, 171 cm, 72 kg) with no lower limb injuries. Written consents have been obtained from all the participants before the experiments. To conduct the experiments, the subject was first fitted to GAREX which was adjusted according to the subject's anthropometric data. The subject performed a trial walk with robotic guidance for 5 minutes, so he could get used to the assisted walk with GAREX. After a rest of 5 minutes, the actual compliance adaptation experiments would be conducted. The subject was requested to behave differently in three experiments with GAREX. In the first experiment, the "Active" case, subjects were required to actively follow the guidance of the exoskeleton to walk in the desired trajectory. The experiment is designed to simulate the rehabilitation training scenario in which a patient makes a good effort to actively participate in the training. In the second experiment, the "Relax" case, subjects were required to try to fully relax the leg attached to the exoskeleton and let GAREX provide the torque needed to produce the desired gait pattern. This experiment was designed to simulate the gait rehabilitation scenario when a patient is not capable of making active participation. In the last experiment, the "Oppose" case, subjects were asked to oppose the guidance as much he could comfortably do, during the swing phase; meanwhile, he was still able to walk on the treadmill safely. This experiment aimed to simulate patients with stiff joints or spasm during robotic rehabilitation. Each of the experiments lasted for 3 minutes and in between two experiments there was a rest period of 3 minutes. In all the experiments, the desired gait cycle period was set to 2.2 seconds.

The experimental results of the three participants were shown in Fig.5 for Subject A, Subject B and Subject C. For comparison purposes, the results of the experiments

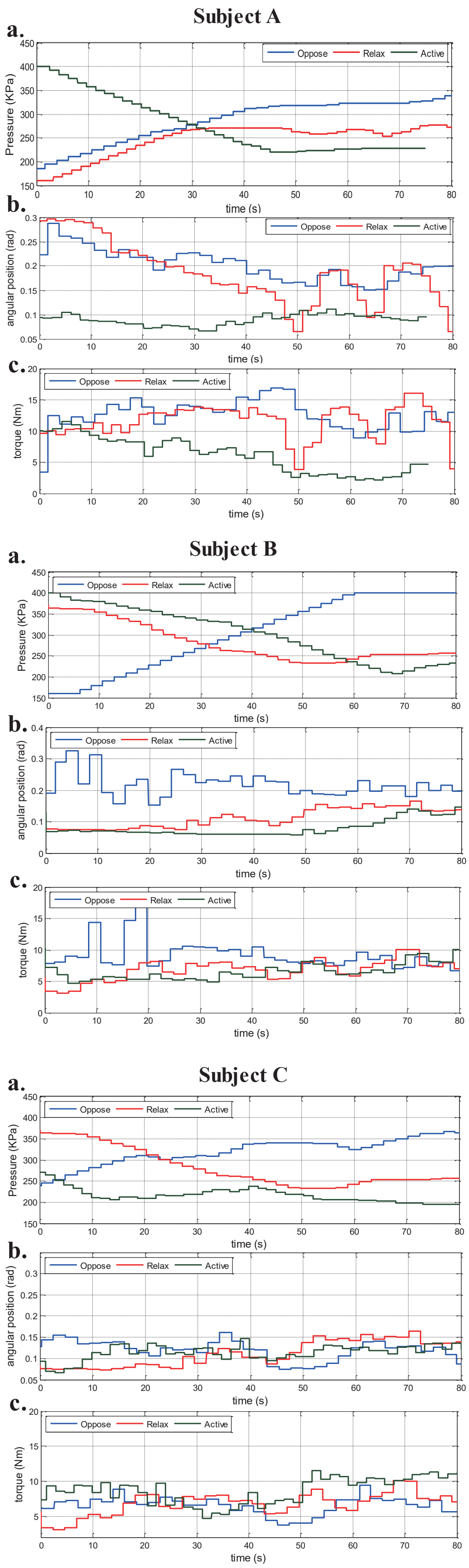

Fig 5. The experimental result plots of three subjects. In all figures: (a) The desired knee joint average PM pressure (measurement of compliance) versus time plots. (b) The gait cycle RMS trajectory error versus time plots. (c) The gait cycle RMS interaction torque versus time plots.

conducted by the same subject are shown in the same figure. Each of the figure contains three subplots. The output of the FLCA controller is represented by the P_{kd} plot. The controller inputs, which are the gait cycle RMS trajectory error and the gait cycle RMS interaction torque, are also shown in the figures. To ensure the readability of the plots, only 80-second segments of experiments are plotted. For each experiment, the starting point of the desired average pressure was chosen differently so the compliance adaptation processes could be visualized.

As stated in the adaptation rule, the compliance is supposed to be high when the active participation by the subject is detected. On the other hand, if the subject is not capable to follow the desired gait pattern. The compliance is supposed to be decreased to constrained subject's lower limb to the desired trajectory. As shown in Fig.5 subplots (a), after stable compliance had been achieved, actively following the desired trajectory resulted in the highest compliances (lowest average PM pressure) for all the subjects. Compared to actively following, the experiments with subjects relaxing their legs attached to the exoskeleton resulted in lower compliance levels. The lowest compliance was resulted by subjects deliberately opposing the robotic guidance. Such experimental results indicate that the control system performed to the overall expectation.

From the gait cycle trajectory error in Fig.5 subplots (b), it can be obtained that the magnitude of the trajectory error is generally positively correlated to the compliance level. However, the correlation is not obvious for the "Oppose" experiments conducted by Subject B and C. There are also relatively large magnitude variations in the "Oppose" experiments conducted by Subject A and Subject B, as well as the "Relax" experiment by Subject A. Different experiments conducted by the same subject were also compared. For Subject A and Subject B, the best overall trajectory tracking performance achieved in "Active" experiments, followed by the "Relax" experiments. The "Oppose" experiments scored the largest overall tracking error. However, for Subject B, no obvious difference in tracking performance could be identified. These results indicated that it is not practical to perform compliance adaptation only based on kinematics feedback.

Compared to the gait cycle RMS trajectory error, as shown in Fig.5 subplots (c), it is even less likely to only use the interaction torque to perform compliance adaption. Besides, there are no obvious differences in τ_{int_k} between the three experimental conditions of the same subject. However, the inter-subject comparison shows some obvious differences. For Subject A, after the compliance levels adaption had been settled, the overall interaction torque in the "Active" experiment is much lower than the other two experiments. For Subject C, the highest interaction torque was achieved by the "Active" experiment.

Through the analysis, it can be concluded that the controller can assess if subjects are actively participating in the trial and adjust the compliance level regardless that different subjects may produce different input patterns when trying to make a similar effort.

The overall control system fore-mentioned in Fig.3 is a cascade control structure. The FLCA controller's output ($\overline{P}_{kd}$) is one of the inputs for the MIMO SM controller. It is necessary to investigate if the MIMO sliding mode controller can track the desired average PM pressures. The tracking results of the three experiments conducted by Subject B are

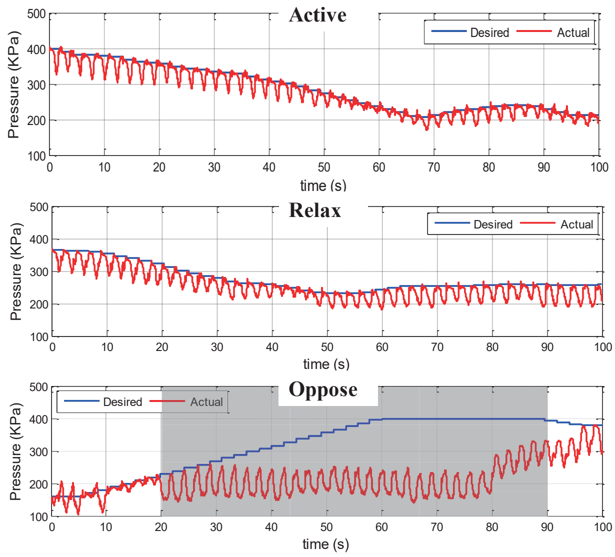

Fig 6. The desired and actual average PM pressures of the knee joint versus time plots for the three experiments conducted by Subject B. (a) "Active" experiment; (b) "Relax" experiment; (c) "Oppose" experiment.

shown in Fig.6. As can be seen from the first two plots of the figure, the system was able to closely track the adapted $\overline{P}_{kd}$. However, for the "Oppose" case, the system was able to track the desired PM pressure for the first 20 seconds. After 20 seconds, the controller was unable to deliver satisfactory tracking performance. For the last five seconds, the control system managed to bring the average PM pressure back to its desired magnitude. The MIMO SM controller tuning could be one of the causes of the suboptimal control system performance. The MIMO SM controller needs to control the angular trajectory and the average PM pressure of an actuated joint simultaneously. Considering the safety and nature of robotic gait rehabilitation, angular trajectory tracking needs to be prioritized among the two control objectives. This was implemented by the tuning parameters that let angular trajectory tracking take the dominant role in the overall control actions. As a result, the large trajectory error in the "Oppose" experiment led to significant control action to drive the knee joint back to its desired position. The control action to maintain the average pressure thus became less effective. However, after the 90-second mark of Fig.6 (c), the desired average pressure started decreasing, which is an indication that the subject's effort of opposing the guidance may have reduced. The angular position tracking could thus also be improved and the better average pressure regulation has resulted.

It can also be observed that the actual average PM pressure oscillated just below the desired value, even when the tracking was effective. Within the same gait cycle, the demand of control action to track the gait trajectory varies. For the knee joint, the trajectory over the swing phase is much more challenging for the controller than the stance phase. The average pressure tracking performance is somehow affected and hence the oscillations happen. Apart from the controller tuning strategy, the limited control system bandwidth could also a cause of imperfect performance.

IV. Discussion

In this study, a fuzzy compliance adaptation controller was integrated with the existing MIMO sliding mode controller to implement the ANN concept with the GAREX system. A fuzzy logic compliance adaption controller is demonstrated to be suitable for this application due to multivariable inputs. It also enables the implementation of the adaptation law based on predefined training principles directly from clinical practice in natural language terms. The fuzzy controller adjusts the knee joint compliance of the exoskeleton based on the subject participation assessment through the gait kinematics and knee joint interaction torque. One of the significant benefits of FLCA controller is that it does not require the model of the exoskeleton or the human biomechanics; therefore, it could be more practical in clinical settings.

The developed FLCA control system was experimentally validated with three healthy subjects. Each subject participated experiment to simulate three different capability/effort levels of patients with gait problems. The experimental results indicated that the FLCA control system was able to distinguish the capability/effort levels and adapt the knee joint compliance of the exoskeleton accordingly. Experimental results also reveal that the MIMO sliding mode controller was able to regulate the average PM pressure of the knee joint to the reference provided by the FLCA controller except when the subject was opposing the robotic guidance to create significant trajectory error.

Although effective compliance adaption has been successfully achieved, there are still potential improvements that could be made to the control system. In terms of the controller implementation, the stance and swing phase of a gait cycle could be distinguished, because the torque s of the two phases are considerably different. It would also be more meaningful to investigate the interaction torque of the two phases separately. The ground reaction force sensor can be used to distinguish the two phases. It can also be utilized together with the 6-axis load cell to more accurately estimate the knee joint interaction torque during the stance phase. With more accurate joint torque mapping over the entire gait cycle the fuzzy controller could thus be updated for better control accuracy.

V. Conclusions and Future Work

To summarize, this study proposes a model-free FLCA controller to form a novel cascade system. To the author's best knowledge, this is the first attempt to implement fuzzy logic-based compliance adaption on rehabilitation robots driven by PM actuators. Experiments were conducted with three healthy subjects and results showed that the FLCA controller could effectively distinguish the capability/effort levels and adapt the knee joint compliance of the exoskeleton accordingly. During experiments in three walking sceneries the maximum angular deviations from desired joint angle trajectories is 0.19 rad. This performance is consistent with the other gait rehabilitation orthoses such as Lokomat, for which the maximum trajectory tracking errors during the position control mode must be less than 15° [24]. The results also indicated FLCA and MIMO sliding mode controllers collaborated well as a system to put the ANN concept into practice with the GAREX.

Further improvements to the experiments are also possible. Interviews with the participants revealed that the "Active" experiments were the easiest to conduct for all of them. They felt walking with GAREX is quite similar to natural walking. All the subjects reported that it is difficult to fully relax the leg attached to GAREX and not participate at all, mainly because it is hard to have the robot support the body weight during the single stance phase on the attached leg without the fear of falling. A possible solution could be the introduction of a bodyweight support system. For the "Oppose" experiments, it was observed that the magnitudes of trajectory error and interaction torque were varied among the subjects, because of their differences in strength. In further studies, it may be worthy to provide visual feedback to the subject during the experiments, so the subjects could better follow the researcher's instructions. This would help produce quantified participation levels of the subject for more in-depth control performance evaluation.

Disclosure statements

The authors declare that there is no conflict of interest.

References

1. Marchal-Crespo, L. and D.J. Reinkensmeyer, *Review of control strategies for robotic movement training after neurologic injury.* Journal of NeuroEngineering and Rehabilitation, 2009. **6**(1): p. 20.
2. Cai, L.L., et al., *Implications of assist-as-needed robotic step training after a complete spinal cord injury on intrinsic strategies of motor learning.* The Journal of neuroscience, 2006. **26**(41): p. 10564-10568.
3. Lotze, M., et al., *Motor learning elicited by voluntary drive.* Brain, 2003. **126**(4): p. 866-872.
4. Kaelin-Lang, A., L. Sawaki, and L.G. Cohen, *Role of voluntary drive in encoding an elementary motor memory.* Journal of neurophysiology, 2005. **93**(2): p. 1099-1103.
5. Zhang, M., T.C. Davies, and S. Xie, *Effectiveness of robot-assisted therapy on ankle rehabilitation - a systematic review.* Journal of NeuroEngineering and Rehabilitation, 2013. **10**: p. 30.
6. Zhang, M., et al., *Adaptive Patient-Cooperative Control of a Compliant Ankle Rehabilitation Robot (CARR) with Enhanced Training Safety.* IEEE Transactions on Industrial Electronics, 2017. **65**(2): p. 1398 - 1407.
7. Yoon, J., et al., *A 6-DOF gait rehabilitation robot with upper and lower limb connections that allows walking velocity updates on various terrains.* IEEE/ASME Transactions on Mechatronics, 2010. **15**(2): p. 201-215.
8. Jezernik, S., G. Colombo, and M. Morari, *Automatic gait-pattern adaptation algorithms for rehabilitation with a 4-DOF robotic orthosis.* IEEE Transactions on Robotics and Automation, 2004. **20**(3): p. 574-582.
9. Riener, R., et al., *Patient-cooperative strategies for robot-aided treadmill training: first experimental results.* Neural Systems and Rehabilitation Engineering, IEEE Transactions on, 2005. **13**(3): p. 380-394.
10. Hussain, S., S.Q. Xie, and P.K. Jamwal, *Adaptive Impedance Control of a Robotic Orthosis for Gait Rehabilitation.* Cybernetics, IEEE Transactions on, 2012. **43**(3): p. 1025-1034.
11. Hussain, S., S.Q. Xie, and P.K. Jamwal, *Control of a robotic orthosis for gait rehabilitation.* Robotics and Autonomous Systems, 2013. **61**(9): p. 911-919.
12. Veneman, J.F., et al., *Design and Evaluation of the LOPES Exoskeleton Robot for Interactive Gait Rehabilitation.* Neural Systems and Rehabilitation Engineering, IEEE Transactions on, 2007. **15**(3): p. 379-386.
13. Banala, S.K., S.K. Agrawal, and J.P. Scholz. *Active Leg Exoskeleton (ALEX) for Gait Rehabilitation of Motor-Impaired Patients*. in *Rehabilitation Robotics, 2007. ICORR 2007. IEEE 10th International Conference on*. 2007.
14. Banala, S.K., et al., *Novel Gait Adaptation and Neuromotor Training Results Using an Active Leg Exoskeleton.* IEEE/ASME Transactions on Mechatronics, 2010. **15**(2): p. 216-225.
15. Tran, H.T., et al., *Evaluation of a Fuzzy-Based Impedance Control Strategy on a Powered Lower Exoskeleton.* International Journal of Social Robotics, 2016. **8**(1): p. 103-123.
16. Chang, M.-K., *An adaptive self-organizing fuzzy sliding mode controller for a 2-DOF rehabilitation robot actuated by pneumatic muscle actuators.* Control Engineering Practice, 2010. **18**(1): p. 13-22.
17. Xie, S.Q. and P.K. Jamwal, *An iterative fuzzy controller for pneumatic muscle driven rehabilitation robot.* Expert Systems with Applications, 2011. **38**(7): p. 8128-8137.
18. Yang, J., et al., *Adaptive control with a fuzzy tuner for cable-based rehabilitation robot.* International Journal of Control, Automation and Systems, 2016. **14**(3): p. 865-875.
19. Ayas, M.S. and I.H. Altas, *Fuzzy logic based adaptive admittance control of a redundantly actuated ankle rehabilitation robot.* Control Engineering Practice, 2017. **59**: p. 44-54.
20. Cao, J., S.Q. Xie, and R. Das, *MIMO Sliding Mode Controller for Gait Exoskeleton Driven by Pneumatic Muscles.* IEEE Transactions on Control Systems Technology, 2017. **PP**(99): p. 1-8.
21. Dao, Q.-T. and S.-i. Yamamoto, *Assist-as-needed control of a robotic orthosis actuated by pneumatic artificial muscle for gait rehabilitation.* Applied Sciences, 2018. **8**(4): p. 499.
22. Hussain, S., et al., *Assist-as-needed control of an intrinsically compliant robotic gait training orthosis.* IEEE Transactions on Industrial Electronics, 2016. **64**(2): p. 1675-1685.
23. Yeh, T.-J., et al., *Control of McKibben pneumatic muscles for a power-assist, lower-limb orthosis.* Mechatronics, 2010. **20**(6): p. 686-697.
24. Riener, R., et al., *Patient-cooperative strategies for robot-aided treadmill training: first experimental results.* IEEE Trans Neural Syst Rehabil Eng, 2005. **13**(3): p. 380-94.
25. Mamdani, E.H. and S. Assilian, *An experiment in linguistic synthesis with a fuzzy logic controller.* International journal of man-machine studies, 1975. **7**(1): p. 1-13.